# Computational and Experimental Inverse Problem Approach for Determination of Time Dependency of Heat Flux...

**Article** · December 2017

DOI: 10.1016/j.procir.2017.03.204



**5 authors**, including:

Volodymyr Bushlya
Lund University
**46** PUBLICATIONS **271** CITATIONS
SEE PROFILE

Oleksandr Gutnichenko
Lund University
**16** PUBLICATIONS **31** CITATIONS
SEE PROFILE

Available online at www.sciencedirect.com

ScienceDirect

Procedia CIRP 58 (2017) 122 – 127

www.elsevier.com/locate/procedia

16th CIRP Conference on Modelling of Machining Operations

# Computational and experimental inverse problem approach for determination of time dependency of heat flux in metal cutting

V. Kryzhanivskyy[a,b], V. Bushlya[a,*], O. Gutnichenko[a], R. M'Saoubi[c], J.-E. Ståhl[a]

[a]*Division of Production and Materials Engineering, Lund University, Ole Römers väg 1, Lund, 22100, Box-118, Sweden*
[b]*Department of Computer Sciences, Zhytomyr State Technological University, Chernyakhovsky, 103, Zhytomyr, 10013, Ukraine*
[c]*Seco Tools (U.K) Ltd., Springfield Business Park , Alcester, Warwickshire, B49 6PU , UK*

* Corresponding author. Tel.: +46-046-222-4607; fax: +46-046-222-8504. E-mail address: volodymyr.bushlya@iprod.lth.se

**Abstract**

This study develops the method for solution of inverse heat conduction problem applied to metal cutting. The proposed method operates with a selection procedure involving iterative solutions of heat forward problem. In such formulation, it allows avoiding difficulties associated with ill-posed inverse problems inherent to conventional formulations. Inverse heat problem was transformed into constrained optimization problem via objective function which metrizes the difference between FE and experimental data. Specially designed solid HSS cutting tool with embedded thermocouples was manufactured. The method was validated for the case of orthogonal machining of 6061 aluminum alloy. The numerical simulations were performed with the help of COMSOL Multiphysics and MATLAB scripts. Heat flux exhibits descending trend over the time of the cutting test and closely follows hyperbola function behavior with the average value of $q$ = 4.6 MW/m$^2$.


Peer-review under responsibility of the scientific committee of The 16th CIRP Conference on Modelling of Machining Operations

*Keywords:* Tool temperature; inverse problem approach; heat flux.

## 1. Introduction

Thermal phenomena in metal cutting play an important role in questions of machining efficiency and quality of the produced parts [1]. A number of different techniques and approaches for measurement and modelling of the cutting temperature exists [2]. Modelling offers an advantage of 3D information on temperature and its distribution, but carries several uncertainties related to input parameters: material models, power and distribution of heat sources, boundary conditions, etc.

An approach combining computational and experimental techniques, in the so-called inverse heat problem formulation, enables reconstructing such unknown input parameters [3]. However, such inverse problems are ill-posed in the sense of J. Hadamard [4], which may return non-unique solution. A number of so-called regularization methods have been proposed to overcome this difficulty [5]. The basic idea of the regularization is to involve additional information on the behavior of the inverse problem solution and therefore narrow down the set of solutions. Thus, the specifics of each individual inverse problem determine the possibility of obtaining this additional information and selection of methods for solution set narrowing [6]. This means that no universal method for inverse problem solution exists.

Several approaches have been applied in metal cutting. In particular, an estimation of heat flux and temperature in a cutting tool during turning was obtained with the help of a two-stage procedure [7]. First, model coefficients were identified via a special apparatus permitting control over heat flux and tool tip temperature. Second, the inverse heat conduction problem in real cutting process is solved using three of the following techniques: exact matching method, sequential function specification method, and sequential regularization method.

An innovative approach based on iterative Newton–Raphson procedure was used in order to identify a spatial distribution of the heat flux into the tool and heat transfer coefficient between


Peer-review under responsibility of the scientific committee of The 16th CIRP Conference on Modelling of Machining Operations
doi:10.1016/j.procir.2017.03.204

the tool and the environment in orthogonal turning [8]. This iterative method minimizes the error defined by the difference between calculated and experimental temperatures.

The inverse algorithm utilizing the steepest descent method and measured temperatures [9] was applied for reconstruction of heat flux when drilling titanium [10]. A special algorithm for gradient identification was developed.

A 3D heat conduction inverse procedure based on Duhamel superposition integral was used for investigation of heat flux [11] and tool–chip thermal conductance [12]. However, this procedure operates only with temperature-independent material properties.

Brito R.F. et al. [13] proposed the use of a nonlinear inverse problem technique to estimate the heat flux and the temperature distribution in a cutting tool in turning operation. Their inverse approach is based on the specification function technique [4]. It however requires pre-definition of sensitivity coefficients [14] and time-steps [4] for each machining case.

The general feature of these inverse problem techniques is their dependence on regularization approaches which must be reformulated or re-tuned for each new machining case or even for each single iteration. This is characteristic for all ill-posed problems [15, 16].

The paper presents the developed inverse problem method operating with selection procedure based on iterative solution of heat forward problem. In such formulation, it is a well-posed problem. The method was validated for the case of orthogonal machining of 6061 aluminum alloy.

## 2. Methods

To achieve this objective, a special experimental setup was built. Its design helped to avoid the uncertainties associated with an additional heat source, due to wear, as well as the uncertainties due to thermal contact conditions between the insert, anvil and clamp plate. Then the finite element model of the setup and the software to implement the method of selection were developed.

### *2.1. Experimental setup*

Orthogonal cutting tests were performed on a 70-kW SMT 500 CNC lathe, which allows maintaining constant cutting speed as the diameter of the workpiece reduced during turning. The operation involved machining 6061 aluminum alloy disk of 470 mm in diameter and 4 mm in thickness. The scheme of the experimental setup is presented in Fig. 1.

The cutting tool was manufactured as a solid rectangular bar with 25 mm square cross-section and 180 mm length. The tool was ground to zero rake angle and 7 degrees clearance angle. Tool material was a high speed steel Vanadis® 23 SuperClean (Uddeholm) [17] hardened to 64 HRC. Fine holes for the placement of thermocouples were obtained via sink EDM with the diameter of each hole of 0.4 mm (Fig. 2). The depth of the holes was 12.5 mm, which corresponds to the tool center plane.

Eight thermocouples, in total, were placed inside the tool holder. Fine-gauge Kapton insulated thermocouples (Omega Engineering) SC-KK-K-40-1M with the wire diameter of 80 μm, providing a fast-response, were used for the temperature registration in respective positions (Fig. 2). Temperature signal acquisition was realized through MATLAB (version 8.5) through NI9213 high-density thermocouple module (National Instruments). A high thermal conductivity silicone paste Omegatherm 201, up to 250°C of short-term exposure, was filled into the holes to ensure proper contact conditions following the recommendations [2]. A collet was manufactured, specially designed to ensure proper thermal contact between the collet and the tool (Fig. 1 and Fig. 3). Thermal paste was also applied on the contacting interfaces there. The experimental setup also included a three-component dynamometer (Kistler 9129AA) for cutting force registration.

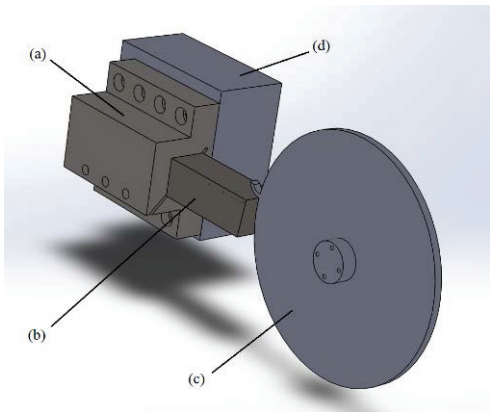


Fig. 1. The scheme of the experimental setup (a) collet; (b) solid HSS cutting tool, (c) workpiece, (d) dynamometer.

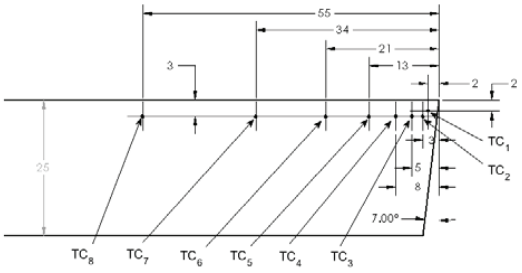


Fig. 2. The placement of holes for thermocouples.

The photograph of the setup and equipment assembly is given in Fig. 3.

Table 1. Thermal properties of the tool material [17].

| Temperature range (°C) | $20 \le u \le 400$ | $400 \le u \le 600$ |
|---|---|---|
| Density, $\rho$ | -0.28947 $u$ + 7985.8 | -0.32500 $u$ + 8000 |
| Thermal conductivity, $k$ | 0.010526 $u$ + 23.789 | -0.005 $u$ + 30 |
| Specific heat, $c_p$ | 0.23684 $u$ + 415.26 | 0.45 $u$ + 510 |

The orthogonal cutting tests was carried at cutting speed $v_c$ = 150 m/min and feed $f$ = 0.2 mm/rev. The actual dimensions of the tool-chip contact area were determined *post mortem* on the tool rake as shown in Fig. 5. The temperature-dependent thermal properties of the cutting tool materials are summarized in Table 1. The cutting test has been performed under dry cutting conditions.

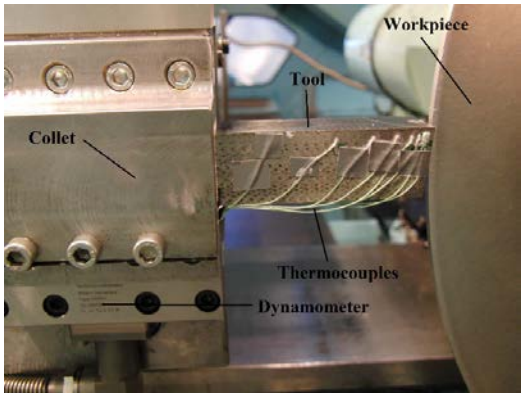


Fig. 3. Photograph of the experimental setup.

### 2.2. Boundary value problem

**Nomenclature**

| | |
|---|---|
| $q$ | heat flux, W/m$^2$ |
| $t$ | time, sec |
| $c_p$ | specific heat, J/(kg K) |
| $k$ | thermal conductivity, W/(m K) |
| $u$ | temperature, $^o$C |
| $h$ | heat transfer coefficient, W/(m$^2$ K) |
| $\rho$ | density, kg/m$^3$ |
| $T$ | modelling time, sec |

Heat transfer equation (Eq. 1) with appropriate boundary (Eq. 2 and Eq. 3) and initial (Eq. 4) conditions are used as the mathematical description of heat distribution in solid.

$$div(k(u)\ grad\ u) = \rho(u)c_p(u)\frac{\partial u}{\partial t} \quad (1)$$

$$-k(u)\frac{\partial u}{\partial n} = q(t) \quad (2)$$

$$-k(u)\frac{\partial u}{\partial n} = h(u_{ext} - u) \quad (3)$$

$$u\big|_{t=0} = u_{ext} \quad (4)$$

where $u_{ext}$ is the temperature of the surroundings, $q(t)$ is a heat flux into the cutting tool assumed to be time dependent [7, 18] and applied on the tool-chip contact area (Fig. 4). The dimensions of the area were determined experimentally and shown in Fig. 5. Eq. 2 is the boundary condition on tool-chip interface, and Eq. 3 is the boundary condition on the other surfaces exposed to the surroundings. All the faces the cutting tool, except for the tool-chip interface, were exposed to a constant convection with heat transfer coefficient, $h$ = 10 W/(m$^2$K) [19].

### 2.3. Finite element model

The forward calculations for above-mentioned boundary value problem (Eq. 1-4) are performed using COMSOL Multiphysics. Heat Transfer in Solids module in time-dependent mode was used. The 3D nonlinear thermal model was built on the basis of imported geometry from CAD model built in SolidWorks.

The geometry of contact zone and mesh are shown in Fig. 4. Due to the small contact area on the tool-chip contact zone and high temperature gradients within the area, the appropriate meshing is needed. The default triangular mesh resulted in the squeezed tetrahedral elements near the cutting zone. That is why the domain of interest was divided into 6 subdomains in order to arrive at a reliable mesh. A combination of prismatic and tetrahedral types of mesh were used in different subdomains to adapt the mesh to measured dimensions of tool – chip contact area (Fig. 4). Parameters of mesh: number of elements 165899, average element quality 0.6522, minimal element size 0.38 mm, average growth rate 1.634.

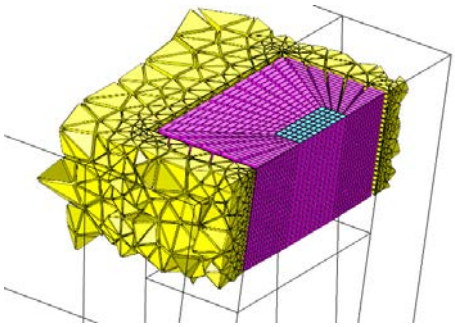

Fig. 4. Meshing around the cutting edge and on the tool – chip contact area.

### 2.4. Inverse problem technique

As aforementioned, the inverse technique adopted in this paper is the method of selection [6]. In order to implement the selection method, the COMSOL model was transformed into MATLAB function with a heat flux $q(t)$ as a variable. This function (1) creates a COMSOL model class in MATLAB workspace, (2) establishes LiveLink to the COMSOL server and (3) sets appropriate model attributes values. Upon completed COMSOL study, the calculated temperatures in the spatial locations of thermocouples are imported into MATLAB workspace where they are compared to the measured ones. This implementation of the modelling environment, built around the combination of COMSOL Multiphysics and MATLAB, has proven to be flexible and easy to maintain.

The comparison is then subjected to the optimization procedure which searches for a heat flux $q(t)$ that minimizes the objective function shown in Eq. 5.

$$f[q(t)] = \left( \sum_{i=1}^{m} \int_{0}^{T} \left( u_i^{mes} - u_i^{calc}(q(t)) \right)^2 dt \right)^{\frac{1}{2}} \quad (5)$$

where $m$ is the number of thermocouples, $u_i^{mes}$ and $u_i^{calc}$ are temperatures measured and calculated in the position of $i$-th thermocouple.

The heat flux $q(t)$ has physical boundaries with the upper limit of the total power consumed during the cutting process and lower limit of zero. These can be expressed as inequalities:

$$0 \le q(t) \le \frac{P}{S} \quad (6)$$

where $P$ is the total power, $S$ is the tool-chip contact area.

## 3. Results and discussion

The chip-tool contact area $S$ has been measured upon the end of the cutting process with the optical microscopy. Leica MZ16 stereomicroscope was used for the determination of the area as shown in Fig. 5. The width of the contact is $b$ = 4.6 mm and the length of contact $l_r$ = 1.9 mm. The cutting process lasted for 45 sec. After this time, the cutting was stopped and the tool was disengaged. The increase of the tool-chip contact from zero, at the moment of engagement, to the full length $l_r$, during the first workpiece revolution, is also implemented in the FE model.

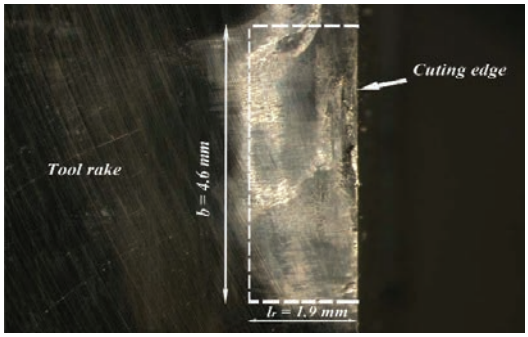


Fig. 5. Tool-chip contact area on the rake.

Cutting forces have been simultaneously recorder during the machining. The measured cutting force component $F_c$ is shown in Fig. 6.

To compute the total power consumed in a cutting process, the cutting forces parallel to the speed directions need to be measured [1]. In the current orthogonal machining study the power equals to:

$$P = F_c v_c + F_f v_f \quad (7)$$

where $F_c$, $F_f$ and $v_c$, $v_f$ are orthogonal components of cutting force and speed respectively. In the present case $v_c >> v_f$. This enables us to disregard the feed component of the cutting force. Then, the total cutting power $P \approx v_c F_c$ = 2.5[m/s]×1000[N] = 2.5 kW.

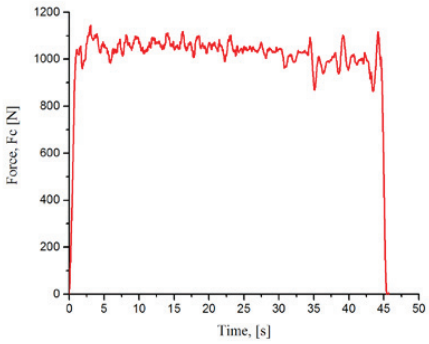


Fig. 6. Recorded cutting force component $F_c$.

The cutting tool is a solid body, which makes it possible to avoid the uncertainties in thermal contact encountered in a conventional toolholder assembly (insert, anvil, clamp plate, etc.). The tool and workpiece materials, as well as cutting conditions, were selected to prevent formation of flank wear and thus avoid an additional heat source on the flank [20]. For such design of experiment only one heat source on the rake is present during the machining.

But, another uncertainty is the spatial distribution of the heat flux over the contact area on the rake (Fig. 5). Uniform [8] and exponential [21] distributions of the heat flux on the rake are reported. Test calculations of the finite element model (Fig. 4) for these different distributions have shown misinterpretation of the calculated temperatures can reach significant values for thermocouples TC1 and TC2 (Fig. 2). Modelling data for the locations at all other thermocouples TC3-TC8 are not sensitive to the spatial heat flux distribution on the rake. Therefore, readings of thermocouples TC1 and TC2 are not taken into account while minimizing the objective function (Eq. 5).

Time-dependency of the heat flux $q(t)$ (Eq. 2) has been reported to be constant over the tool engagement time [8], to rise from zero to a certain asymptotic value [7, 11], and to drop down to an asymptotic value [10]. It is well known that the chip reaches its maximum temperature within a short period of time after the tool engagement. Yet, the temperature value itself is unknown. In terms of boundary conditions for the tool, this corresponds to the Dirichlet condition. At the same time, this Dirichlet condition defines the characteristic behavior of the heat flux through this chip-tool boundary. At the initial time moment, it defines a threshold (Heaviside step function) between the chip temperature at the boundary and the temperature inside the tool body. Theoretically it means that the heat flux at this initial moment equals infinity, because it is proportional to the temperature difference between the hot chip and the cold tool. Further into the cutting process, the heat flux ought to drop rapidly at first, and then decrease at a slower rate.

Such theoretical reasoning allows us to assume the descending time-dependency of the heat flux. Such behavior can be approximated by a power function of the following form:

$$q(t) = \frac{d_1}{t^{d_2}} \tag{8}$$

where $d_1$, $d_2$ are unknown parameters.

One can note that at time moment $t = 0$, this function (Eq. 8) returns infinity. Heat flux was kept constant during the time interval up to 0.05 sec due to impossibility of modelling infinite heat flux. Heat flux value equal to $q$ (0.05) is then followed by the function described in Eq. 8.

Because the differential properties of Eq. 5 are not investigated in this paper, then the use of derivative free method is applied to this optimization problem. The efficiency of such derivative free methods depends on the commensurability in the magnitude of parameters $d_1$ and $d_2$. For $d_1$ of order $\approx 10^6$ W/m$^2$ [8] the difference to $d_2$ is extreme. Therefore, it is justified to parametrize Eq. 8 via two characteristic points $p_1$ and $p_2$ (Fig. 7).

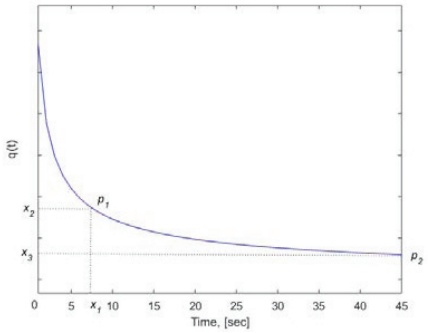


Fig. 7. The behavior of the heat flux function on time.

The parameters $d_1$ and $d_2$ can then be expressed in terms of the coordinates $x_1$, $x_2$, $x_3$ (Fig. 7):

$$d_2 = \ln\left(\frac{x_2}{x_3}\right) / \left(\ln(x_1) - \ln T\right) \tag{9}$$

$$d_1 = \frac{x_2}{x_1^{d_2}} \tag{10}$$

Now the objective function (Eq. 5) becomes dependent on three variables $x_1$, $x_2$, $x_3$:

$$f[x_1, x_2, x_3] = \left( \sum_{i=1}^{m} \int_0^T \left( u_i^{mes} - u_i^{calc}\left(\frac{d_1(x_1, x_2, x_3)}{t^{d_2(x_1, x_2, x_3)}}\right)\right)^2 dt \right)^{\frac{1}{2}} \tag{11}$$

The model constraints (Eq. 6) should be supplemented by the following inequalities:

$$x_2 > x_3, 0 < x_1 < T. \tag{12}$$

After such transformations, the inverse problem (Eq. 5) is interpreted as the mathematical programming problem with the objective function (Eq. 11) and constraints (Eq. 6) and (Eq. 12).

Derivative free Nelder-Mead method was selected as the most resilient. For this aim the objective function (Eq. 11) and constraints were brought to unconstrained optimization problem with the help of a following penalty function:

$$f_{penal}(x_1, x_2, x_3) = \exp\left(z \cdot (x_1 - x_2)\right) + \exp\left(z \cdot (x_1 - T)\right) + \\ + \exp\left(z \cdot (x_1 - T)\right) + \exp\left(z \cdot (q(t) - P)\right). \tag{13}$$

where $z$ is iteratively increasing penalty parameter.

Nelder-Mead method used in the current study requires an initial starting point. In the computational experiments, multiple starting points were randomly generated. For all starting points, the values of objective function and values of variables $x_1$, $x_2$, and $x_3$ practically coincided. This fact makes it possible to assume that the objective function is unimodal.

The values of parameters found of heat flux are $x_1$ = 5.789 sec, $x_2$ = 4.824 MW/m$^2$, $x_3$= 4.117 MW/m$^2$. The value of the objective function is $f$ = 19.278±0.003.

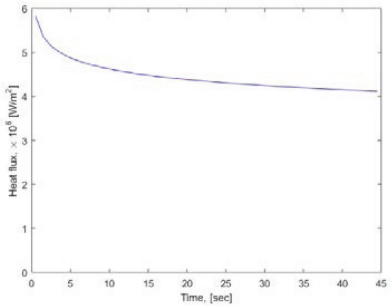


Fig. 8. Computed heat flux behavior.

The corresponding heat flux behavior over the machining time is shown in Fig. 8. Eq. 8 and Fig. 8 show that the average heat flux into the tool equals to 4.6 MW/m$^2$. This value of the flux is in good agreement with values obtained by other techniques [8, 10, 22].

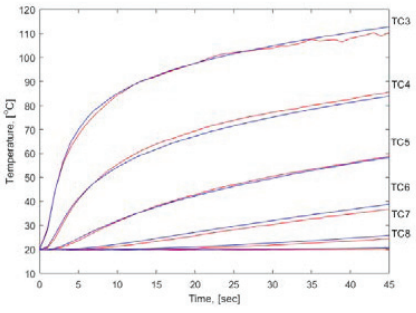


Fig. 9. Experimental (red) and calculated temperatures (blue).

The comparison between calculated and measured temperatures in the same locations of thermocouples TC3-TC8 (Fig. 2) are depicted on Fig. 9.

## 4. Conclusion

This study develops the method for solution of inverse heat conduction problem applied to metal cutting. The proposed method operates with a selection procedure involving iterative solutions of heat forward problem. In such formulation, it allows avoiding difficulties associated with ill-posed inverse problems inherent to conventional formulations.

Inverse heat problem was transformed into constrained optimization problem via objective function which metrizes the difference of FE and experimental data. The argument of the function is the time-dependent heat flux *q(t)* into cutting tool. Introduced penalty function converted this optimization problem into the unconstrained one, addressed via derivative free Nelder-Mead method.

Specially designed solid HSS cutting tool with embedded thermocouples was manufactured. The method was validated for the case of orthogonal machining of 6061 aluminum alloy. Design of the experiment allowed minimizing uncertainties and accounting only for heat flux through the rake. The method returned a descending heat flux behavior with the average value of $q$ = 4.6 MW/m$^2$.

## Acknowledgements

This paper was co-funded by the European Union's Horizon 2020 Research and Innovation Programme under Flintstone2020 project (grant agreement No 689279). It was also co-funded by the research project Sustainable Production Initiative (SPI) involving cooperation between Lund University and Chalmers University of Technology. One of the authors (VK) wishes to acknowledge VINNMER grant (2016-02046) and Visby scholarship by Swedish Institute.

## References

[1] Stahl J-E. Metal cutting: theories and models. Fagersta: SECO Tools; 2012.
[2] Davies MA, et al. On the measurement of temperature in material removal processes. CIRP Ann 2007; 56: 581-604.
[3] Orlande HRB, et al. Thermal measurements and inverse techinques. New York: CRC Press, Taylor & Francis Group; 2011.
[4] Beck JV, Blackwell B, Clair CRSt. Inverse Heat Conduction: Ill-Posed Problems. New-York: A Wiley-Interscience publication; 1985.
[5] Engl HW. Inverse problems and their regularization. In: Computational Mathematics Driven by Industrial Problems. Berlin–New York: Springer; 1999.
[6] Tikhonov AN, Arsenin VY. Solution of Ill-posed Problems. Washington: Winston & Sons; 1977.
[7] Battaglia JL, Batsale JC, Estimation of heat flux and temperature in a tool during turning. Inverse Problems in Engineering 2000; 8: 435-456.
[8] Yvonnet J, et al. A simple inverse procedure to determine heat flux on the tool in orthogonal cutting. Int J of Machine Tools & Manufacture 2006; 46:820–827.
[9] Huang C-H, Lo H-C, A three-dimensional inverse problem in predicting the heat fluxes distribution in the cutting tools. Numerical Heat Transfer 2005; Part A, 48:1009–1034.
[10] Huang C-H, et al. A three-dimensional inverse problem in estimating the applied heat flux of a titanium drilling – Theoretical and experimental studies. Int J of Heat and Mass Transfer 2007; 50: 3265–3277.
[11] Norouzifard V, Hamedi M. A three-dimensional heat conduction inverse procedure to investigate tool–chip thermal interaction in machining process. Int J Adv Manuf Technol 2014; 74:1637–1648.
[12] Norouzifard V, Hamedi M. Experimental determination of the tool–chip thermal contact conductance in machining process. Int J of Machine Tools & Manufacture 2014; 84: 45–57.
[13] Brito RF, et al. Experimental investigation of thermal aspects in a cutting tool using COMSOL and inverse problem. Applied Thermal Engineering 2015; 86:60-68.
[14] Samadi F, at al. Estimation of heat flux imposed on the rake face of a cutting tool: A nonlinear, complex geometry inverse heat conduction case study, Int Commun. in Heat and Mass Transf. 2012; 39:298–303.
[15] Morozov VA, Stessin M. Regularization Methods for Ill-posed problem, CRC Press, Boca Raton, FL, 1992.
[16] Morozov VA. Method for Solving Incorrectly Posed Problems, Springer, Verglad, 1984.
[17] http://www.uddeholm.com/files/PB_Uddeholm_vanadis_23_english.pdf
[18] Carvalho SR, et al. Temperature determination at the chip–tool interface using an inverse thermal model considering the tool and tool holder. J of Materials Processing Technology 2006; 179: 97–104.
[19] Kryzhanivskyy V, et al. Modelling and Experimental Investigation of Cutting Temperature when Rough Turning Hardened Tool Steel with PCBN Tools. Procedia CIRP 2015; 31: 489 – 495.
[20] Kryzhanivskyy V, et al. Influence of Tool Material and Tool Wear on Tool Temperature in Hard Turning reconstructed via Inverse Problem Solution. *Accepted*. Journal of Superhard Materials.
[21] Santos MR, et al. Analyses of Effects of Cutting Parameters on Cutting Edge Temperature Using Inverse Heat Conduction Technique. Mathematical Problems in Engineering 2014; Article ID 871859.
[22] Battaglia J-L, Kusiak A. Estimation of heat fluxes during high-speed drilling. Int J Adv Manuf Technol 2005; 26: 750–758.